

Optimization and Growth in First-Passage Resetting

B. De Bruyne

Perimeter Institute, 31 Caroline Street North, Waterloo, ON, N2L 2Y5, Canada
LPTMS, CNRS, Univ. Paris-Sud, Université Paris-Saclay, 91405 Orsay, France

J. Randon-Furling

SAMM, Université Paris 1 – FP2M (FR2036) CNRS, 75013 Paris, France
Department of Mathematics, Columbia University, New York, NY 10027, USA
MSDA, Mohammed VI Polytechnic University, Ben Guerir 43150, Morocco

S. Redner

Santa Fe Institute, 1399 Hyde Park Rd., Santa Fe, New Mexico 87501, USA

Abstract. We combine the processes of resetting and first-passage to define *first-passage resetting*, where the resetting of a random walk to a fixed position is triggered by a first-passage event of the walk itself. In an infinite domain, first-passage resetting of isotropic diffusion is non-stationary, with the number of resetting events growing with time as \sqrt{t} . We calculate the resulting spatial probability distribution of the particle analytically, and also obtain this distribution by a geometric path decomposition. In a finite interval, we define an optimization problem that is controlled by first-passage resetting; this scenario is motivated by reliability theory. The goal is to operate a system close to its maximum capacity without experiencing too many breakdowns. However, when a breakdown occurs the system is reset to its minimal operating point. We define and optimize an objective function that maximizes the reward (being close to maximum operation) minus a penalty for each breakdown. We also investigate extensions of this basic model to include delay after each reset and to two dimensions. Finally, we study the growth dynamics of a domain in which the domain boundary recedes by a specified amount whenever the diffusing particle reaches the boundary after which a resetting event occurs. We determine the growth rate of the domain for the semi-infinite line and the finite interval and find a wide range of behaviors that depend on how much the recession occurs when the particle hits the boundary.

1. Introduction

Random walks are ubiquitous in phenomena across a wide range of fields, such as physics, chemistry, finance and social sciences [1–4]. In addition to the applications of the random walk, many useful extensions of the basic model have been developed (see, e.g., [5–8]). Almost a decade ago, the notion of resetting of a random walk was introduced [9–11]. The basic idea of resetting is simplicity itself: at a given rate, a random walk is reset to

its starting point. The rich phenomenology induced by this extension of the random walk has sparked much interest (see, e.g., [9–19]). In the context of search strategies, where the walker is searching for a target at a fixed location, resetting changes the average search time from being infinite (in an infinite domain) to finite [20–23]. Moreover, there exists an optimal resetting rate that minimizes the search time. A very different, but also fruitful concept in the theory of random walks is the notion of a first-passage process [2, 24–26]. Of particular importance is first-passage probability, which is defined as the probability that a walker reaches a specified location for the first time. This notion has many applications where a particular event happens when a threshold is first reached. One such example is a limit order for a stock. When the price of a stock, whose evolution is often modeled as a geometric random walk, first reaches a limit price, this event triggers the sale or the purchase of the stock.

In this work, we combine these disparate notions of first passage and resetting into *first-passage resetting*, in which the particle is reset whenever it reaches a specified threshold. Contrary to standard resetting, the time at which first-passage resetting occurs is defined by the motion of the diffusing particle itself rather than being imposed externally [9–11]. Feller showed that such a process is well defined mathematically and provided existence and uniqueness theorems [27], while similar ideas were pursued in [28]. First-passage resetting was initially treated in the physics literature for the situation in which two Brownian particles are biased toward each other and the particles are reset to their initial positions when they encounter each other [29].

In our work, we first focus on the related situation of a diffusing particle on the semi-infinite line $x \leq L$ that is reset to the origin whenever the particle hits the boundary $x = L$ (Fig. 1). The model studied in [29] corresponds to a drift toward the boundary in our semi-infinite geometry; this setting leads to a stationary state. In contrast, the absence of drift in our model leads to a variety of new phenomena. In particular, the probability distribution for the position of the particle is non-stationary. We also construct two simple path decompositions for first-passage resetting, in which the trajectory of the resetting particle is mapped onto a free diffusion process. This approach provides useful geometrical insights, as well as simple ways to derive the average number of reset events and the spatial probability distribution with essentially no calculation.

We then treat first-passage resetting on a finite interval, which has a natural application to reliability theory. Here the particle is restricted to the interval $[0, L]$ where $x = L$ is again the boundary where resetting occurs and the particle is immediately reinjected at $x = 0$ when it reaches $x = L$. We may view this mechanism as characterizing the performance of a driven mechanical system [30–33], with the coordinates $x = 0$ and $x = L$ indicating poor and maximal performance, respectively. While one ideally wants to operate the system close to its maximum performance level ($x = L$), there is a risk of overuse, leading to breakdowns whenever $x = L$ is reached. Subsequently, the system has to be repaired and then restarted from $x = 0$. This dynamics corresponds to resetting that is induced by a first passage to the boundary

$x = L$. We will find the optimal bias velocity that optimizes the performance of the system. We will also investigate additional features of this first-passage resetting, such as a random maintenance delay at each breakdown and resetting in higher dimensions. A preliminary account of some of these results was given in [34].

Finally, we investigate a very different aspect of first-passage resetting where the domain boundary at which resetting occurs moves by a specified amount each time the diffusing particle reaches this boundary. Many features of this moving boundary problem can be readily calculated because of the renewal structure of the theory. For both the semi-infinite and finite interval geometries, we find a variety of scaling behaviors for the motion of the resetting boundary. These behaviors depend on the initial geometry and by how much the boundary moves at each resetting event.

2. First-Passage Resetting in the Semi-Infinite Geometry

In the standard resetting process, reset events occur at a fixed rate r that are uncorrelated with the position of the diffusing particle. In contrast, first-passage resetting directly couples the times at which resetting occurs and the particle position. For first-passage resetting in the semi-infinite line geometry, the particle starts at $x(0) = 0$ and freely diffuses in the range $x \leq L$ (with $L > 0$). Each time L is reached, the particle is instantaneously reset to the origin (Fig. 1). We are interested in two basic characteristics of the particle motion: the spatial probability distribution of the particle and the time dependence of the number of reset events. To compute these quantities, we rely on the renewal structure of the process, which allows us to first compute the probability for n reset events in a direct way. With this result, as well as the propagator for free diffusion in the presence of an absorbing boundary, we can readily obtain the spatial distribution of the particle and the average number of resets up to a given time.

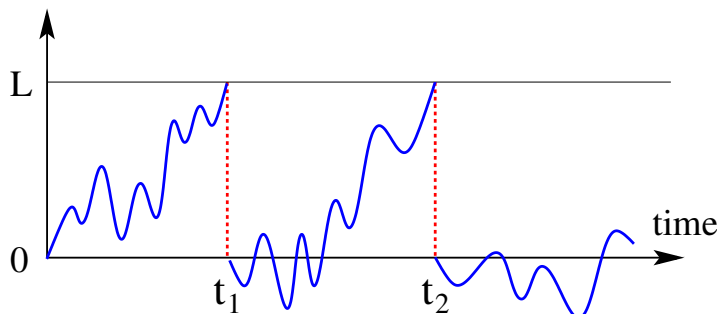


Figure 1. Schematic illustration of first-passage resetting for diffusion on the semi-infinite line $x \leq L$. Each time the particle reaches the threshold L , it is reset to the origin. The times of the resetting events are denoted by t_1, t_2, \dots

2.1. The n^{th} reset probability distribution

Define $F_n(L, t)$ as the probability that the particle resets for the n^{th} time at time t . When $n = 1$, this quantity is the standard first-passage probability for a freely diffusing particle that starts at the origin, to first reach L [25, 26]:

$$F_1(L, t) \equiv F(L, t) = \frac{L}{\sqrt{4\pi Dt^3}} e^{-L^2/4Dt}.$$

For the particle to reset for the n^{th} time at time t with $n > 1$, the particle must reset for the $(n - 1)^{\text{th}}$ time at some earlier time $t' < t$, and reset one more time at time t . Because the process is renewed at each reset, $F_n(L, t)$ is formally given by the renewal equation

$$F_n(L, t) = \int_0^t dt' F_{n-1}(L, t') F_1(L, t - t'), \quad n > 1. \quad (1a)$$

The convolution structure of Eq. (1a) lends itself to a Laplace transform analysis. The corresponding equation in the Laplace domain is simply:

$$\tilde{F}_n(L, s) = \tilde{F}_{n-1}(L, s) \tilde{F}_1(L, s) = \tilde{F}_1(L, s)^n, \quad (1b)$$

where quantities with tildes denote Laplace transforms. Using the Laplace transform of the first-passage probability:

$$\tilde{F}_1(L, s) = \int_0^\infty dt F_1(L, t) e^{-st} = e^{\sqrt{sL^2/D}} \equiv e^{-\ell},$$

where we define the scaled coordinate $\ell \equiv \sqrt{s/D} L$ henceforth, then Eq. (1b) becomes

$$\tilde{F}_n(L, s) = e^{-n\ell}.$$

Notice that $\tilde{F}_n(L, s)$ has the same form as $\tilde{F}_1(L, s)$ with $L \rightarrow nL$. That is, the time for a diffusing particle to reset n times at a fixed boundary $x = L$ is the same as the time for a freely diffusing particle to first reach $x = nL$.

In hindsight, this equivalence between the first-passage probability to $x = nL$ and the n^{th} -passage probability to $x = L$ with resetting at $x = L$ is self evident. As indicated in Fig. 2 for the case $n = 3$, a first-passage path from 0 to $3L$ is composed of a first-passage path from 0 to L , followed by a first-passage path from L to $2L$, and finally a first-passage path from $2L$ to $3L$. Resetting causes each of these three segments to (re)start from the origin. Thus the point $x = L$ is first reached for the third time after resetting by these displaced paths.

2.2. Spatial probability distribution

We now compute the probability distribution of the diffusing particle at time t , $P(x, t)$, on the semi-infinite line $x \leq L$ under the influence of first-passage resetting.

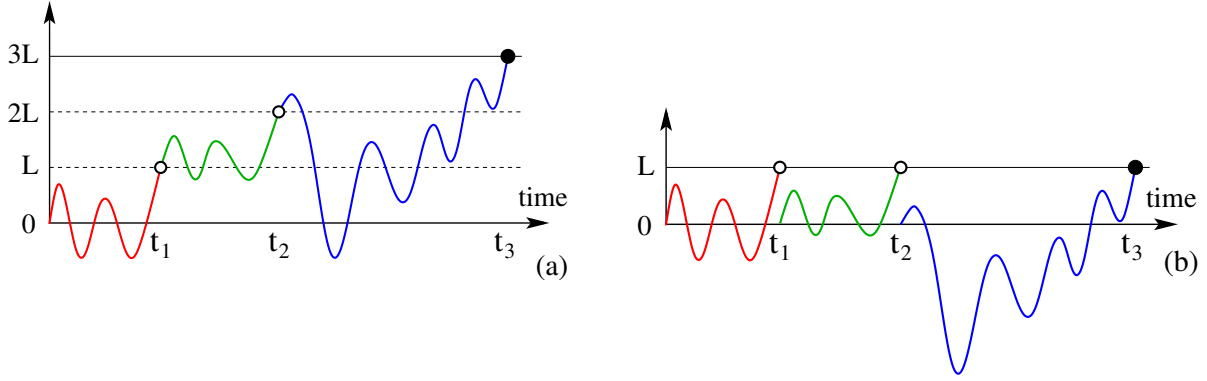


Figure 2. Relation between a first-passage path to $x = 3L$ and a third-passage path to $x = L$, with resetting each time $x = L$ is reached. The green and blue paths in (b) have merely been shifted vertically downward by L and $2L$ compared to (a), respectively.

This distribution can be obtained in several ways. Here we make use of the path transformation discussed above for the derivation of the n^{th} passage probability (see Fig. 2). (A calculational approach based on Laplace transforms that relies on the renewal structure of the process is given in Appendix A.) When the walker is at position $x \in [0, L]$ at time t and has experienced exactly n resets, this is equivalent to a free particle being at position $x + nL$ without having reached level $(n + 1)L$. As a result, the corresponding probability is that of a free particle with position $x(t) = x + nL$ and running maximum position $M(t) < (n + 1)L$; the latter is defined by $M(t) = \max_{t' \leq t} x(t')$. The joint distribution of the position and maximum, $x(t) = x$ and $M(t) = m$, is given by

$$\Pi(x, m, t) = \frac{2m - x}{\sqrt{4\pi D^3 t^3}} e^{-(2m-x)^2/4Dt}. \quad (2)$$

This formula was established by Lévy [35, 36] and it can be derived by using the reflection property of Brownian motion. From this joint probability, we find that

$$\begin{aligned} P(x, t) &= \sum_{n \geq 0} \text{Prob}(M(t) < (n + 1)L \text{ and } x(t) = x + nL) \\ &= \sum_{n \geq 0} \int_{x+nL}^{(n+1)L} dm \Pi(x + nL, m, t) \\ &= \frac{1}{\sqrt{4\pi Dt}} \sum_{n \geq 0} \left[e^{-(x+nL)^2/4Dt} - e^{-[x-(n+2)L]^2/4Dt} \right], \quad 0 < x \leq L. \end{aligned} \quad (3)$$

While this expression is exact, it is not in a convenient form to determine its long-time behavior. However, the long-time limit of $P(x, t)$ is simple to obtain by expanding its Laplace transform (see [34]) for small s ,

$$\tilde{P}(x, s) \simeq \frac{1}{\sqrt{Ds}} \frac{L - x}{L} \quad 0 \leq x \leq L, \quad s \rightarrow 0, \quad (4a)$$

from which the inverse Laplace transform is

$$P(x, t) \simeq \frac{1}{\sqrt{\pi Dt}} \frac{L - x}{L} \quad 0 \leq x \leq L, \quad t \rightarrow \infty. \quad (4b)$$

The linear x dependence arises from the balance between the diffusive flux that exits at the reset point $x = L$ and this same flux being re-injected at $x = 0$.

For $x < 0$, the integral in the second line of (3) ranges from nL to $(n + 1)L$ rather than from $x + nL$. This leads to

$$\begin{aligned} P(x, t) &= \frac{1}{\sqrt{4\pi Dt}} \sum_{n \geq 0} \left[e^{-(x-nL)^2/4Dt} - e^{-[x-(n+2)L]^2/4Dt} \right] \\ &= \frac{1}{\sqrt{4\pi Dt}} \left[e^{-x^2/4Dt} + e^{-(x-L)^2/4Dt} \right], \quad x < 0. \end{aligned} \quad (5)$$

Thus the probability distribution is merely the sum of two Gaussians. In the long-time limit and for $|x|/\sqrt{4Dt} \gg 1$, the factor L in the second term becomes irrelevant and the distribution reduces to that of diffusion on the half line in the presence of a reflecting boundary.

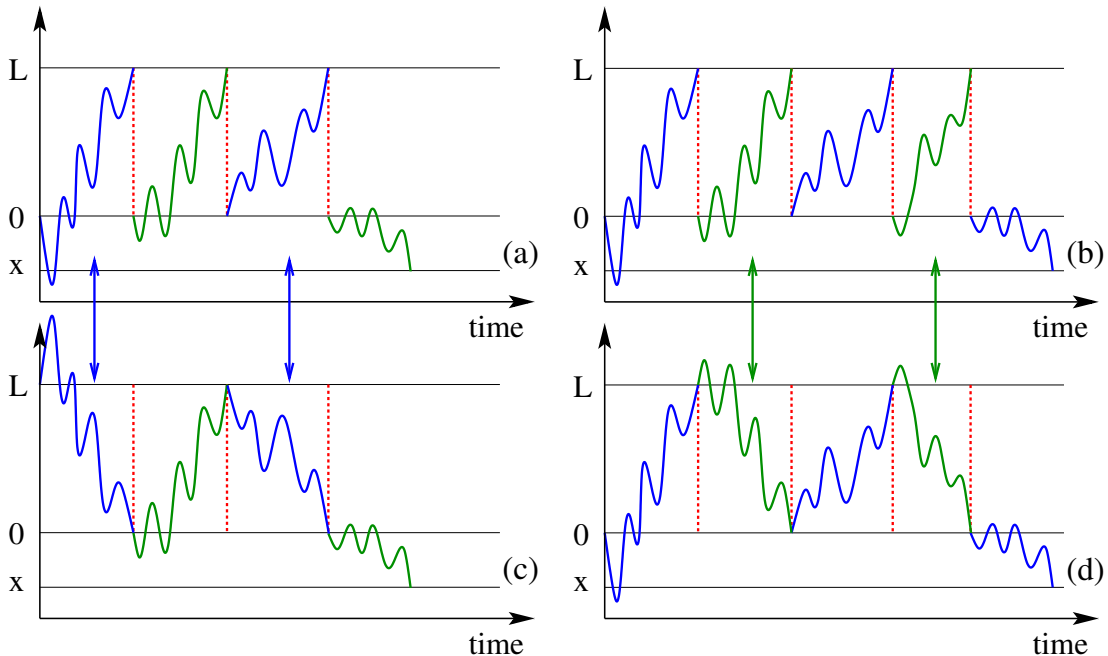


Figure 3. Schematic space-time trajectory of diffusion with first-passage resetting on a semi-infinite line. (a) A path with an odd number of resets is equivalent to (c) a freely diffusing path that starts at $x(t=0) = L$. (b) A path with an even number of resets is equivalent to (d) a freely diffusing path that starts from $x(t=0) = 0$. This equivalence underlies the spatial probability distribution for $x < 0$ in Eq. (5).

An appealing way to obtain the probability distribution (5) is by a path decomposition construction. Consider the original resetting problem and partition all trajectories into those that undergo either an odd or an even number of resets. In the former case, we invert the segments *before* each odd-numbered resetting about the origin and then translate each such segment by a distance $+L$ (blue arrows in Fig. 3(a) & (c)). As shown in this portion of the figure, the resulting trajectory is simply a Brownian path that starts at $x = L$ and propagates freely to its final position x . For a path

that consists of an even number of resetting events, we perform this same inversion and translation on the segments *after* each odd-numbered resetting (green arrows in Fig. 3(b) & (d)). The resulting trajectory is now a Brownian path that starts at the origin and propagates freely to its final position x . It is worth emphasizing that this decomposition applies for any symmetric and continuous stochastic process (provided it is homogeneous and stationary).

2.3. Average number of resets

To find the average number of resets that occur up to time t , we first compute the probability that n resets have occurred during this time. By relying on the path transformation shown in Fig. 2, we find that the probability for exactly n resets to occur by time t equals the probability for a freely diffusing particle to have a running maximum $M(t)$ greater than nL but less than $(n + 1)L$, that is:

$$P(N(t) = n) = \text{Prob}(nL \leq M(t) < (n + 1)L). \quad (6)$$

The distribution of $M(t)$ is known [36–38] and may be readily rederived from (2),

$$P(M(t) = m) = \frac{1}{\sqrt{\pi Dt}} e^{-m^2/4Dt},$$

from which it follows that

$$P(N(t) = n) = \text{erf}\left(\frac{(n + 1)L}{\sqrt{4Dt}}\right) - \text{erf}\left(\frac{nL}{\sqrt{4Dt}}\right), \quad (7)$$

where erf is the Gauss error function.

We can compute the average number of reset events, $\mathcal{N}(t) \equiv \langle N(t) \rangle$, from (7), but it is quicker to use again the mapping with the running maximum of free diffusion. Indeed, writing $\mathcal{M}(t)$ for the average maximum position of a freely diffusing particle up to time t , one has

$$\mathcal{N}(t) L \leq \mathcal{M}(t) < [\mathcal{N}(t) + 1] L. \quad (8)$$

Since $\mathcal{M}(t) = \sqrt{4Dt/\pi}$, we find that the long-time behavior of $\mathcal{N}(t)$ is given by

$$\mathcal{N}(t) \simeq \sqrt{4Dt/\pi L^2}. \quad (9)$$

The resetting process is non-stationary, as the number of reset events grows as \sqrt{t} .

2.4. Biased diffusion

The case where the diffusing particle is biased towards the resetting boundary is equivalent to the model studied by Falcao and Evans [29]. Here we briefly discuss the complementary situation in which the particle is biased away from the resetting boundary, with drift velocity $v < 0$. In the absence of resetting, a particle that starts at the origin eventually reaches $x = L$ with probability $H = e^{-Pe}$ and escapes to

$x = -\infty$ with probability $1 - H$ [24, 25], where $\text{Pe} \equiv vL/2D$ is the Péclet number (the dimensionless bias velocity). When resetting can occur, H now becomes the probability that a resetting event actually happens. Consequently, the probability that the particle resets exactly n times is given by $R_n = H^n(1 - H)$. The average number of resetting events before ultimate escape therefore is [35]

$$\mathcal{N}(t) = \sum_n n R_n = \frac{H}{1 - H} = \frac{1}{e^{\text{Pe}} - 1}. \quad (10)$$

In the limit of $v \rightarrow 0$, the number of resetting events diverges as $\mathcal{N}(t) \simeq 2D/(vL)$. The time between resetting events is known to be L/v [25, 39]. Thus after typically $1/(e^{\text{Pe}} - 1)$ resetting events, each of which requires a time of L/v , the particle escapes to $-\infty$.

We can also compute the spatial probability distribution of the particle when it undergoes biased diffusion with bias velocity of magnitude v . We make use again of the path transformation shown in Fig. 2. For a Brownian particle with drift v , the analog of Eq. (2) is

$$\Pi(x, m, t) = \frac{2m - x}{\sqrt{4\pi D^3 t^3}} e^{-(2m-x)^2/4Dt} e^{\text{Pe}(x/L - \text{Pe} Dt/L^2)}, \quad (11)$$

which leads to

$$P(x, t) = \frac{1}{\sqrt{4\pi Dt}} \sum_{n \geq 0} \left[e^{-(x+nL)^2/4Dt} - e^{-[x-(n+2)L]^2/4Dt} \right] e^{\text{Pe}(x/L + n - \text{Pe} Dt/L^2)}, \quad 0 < x \leq L \quad (12a)$$

and

$$P(x, t) = \frac{1}{\sqrt{4\pi Dt}} \sum_{n \geq 0} \left[e^{-(x-nL)^2/4Dt} - e^{-[x-(n+2)L]^2/4Dt} \right] e^{\text{Pe}(x/L + n - \text{Pe} Dt/L^2)}, \quad x < 0. \quad (12b)$$

In contrast to the driftless case, there is no simplification for the probability distribution when $x < 0$. In particular, the path transformation of Fig. 3 requires symmetry and thus does not hold in the presence of drift.

3. Optimization in First-Passage Resetting

3.1. The finite interval

We now introduce an optimization problem that is induced by first-passage resetting. We envisage a mechanical system whose operating coordinate $x(t)$ lies in the range $[0, L]$. Increasing the value of x corresponds to increasing its level of operation, and it is desirable to run the system as close as possible to its maximum capacity L . However, the system breaks down whenever x reaches L , after which repairs have to be made before the system can restart its operation from $x = 0$. While the dynamics of the operating

coordinate is typically complicated and dependent on multiple parameters, we view the coordinate x as undergoing a drift-diffusion process for the sake of parsimonious modeling. For the system to be close to $x = L$, the drift should be positive. On the other hand, breakdowns of the system are to be avoided because a cost is incurred with each breakdown. This suggests that the drift velocity should be negative. The goal is to determine the optimal operation that maximizes the performance of the system as a function of the cost for each breakdown and the drift velocity. Although the analogy between first-passage resetting and a mechanical system is naive, this formulation allows us to determine the optimal operation in a concrete way.

The basic control parameter is the magnitude of the drift velocity. If the velocity is large and negative, the system is under-exploited because it operates far from its maximum capacity. Conversely, if the velocity is large and positive, the system breaks down often. We seek the optimal operation by maximizing an objective function \mathcal{F} that rewards high performance and penalizes breakdowns. A natural choice for \mathcal{F} is

$$\mathcal{F} = \lim_{T \rightarrow \infty} \frac{1}{T} \left[\frac{1}{L} \int_0^T x(t) dt - C \mathcal{N}(T) \right], \quad (13)$$

where T is the total operation time, $\mathcal{N}(T)$ is the average number of breakdowns within a time T , with T much longer than the mean breakdown time, and C is the cost of each breakdown. As defined, this objective function rewards operation close to the maximum point L and penalizes breakdowns.

We now determine this objective function when the operating coordinate $x(t)$ evolves according to drift-diffusion, with the additional constraint that $x(t)$ is reset to zero whenever x reaches L . Mathematically, we need to solve the convection-diffusion equation with the following additional conditions: (i) a δ -function source at the origin whose magnitude is determined by the outgoing flux $j(x) = -D\partial_x c + vc$ at $x = L$, (ii) a reflecting boundary condition at $x = 0$, and (iii) the initial condition $x(t = 0) = 0$. That is, we want to solve

$$\partial_t c + v\partial_x c = D\partial_{xx} c + \delta(x)(-D\partial_x c + vc)|_{x=L}, \quad (14a)$$

subject to

$$\begin{cases} (D\partial_x c - vc)|_{x=0} = \delta(t) \\ c(L, t) = 0 \\ c(x, 0) = 0 \end{cases} .$$

Here, $c \equiv c(x, t)$ is the probability density for the operating coordinate, the subscripts denote partial differentiation, D is the diffusion coefficient, and v is the drift velocity. Notice that the reflecting boundary condition at $x = 0$ holds *except* at the start of the process to account for the unit input of flux at $t = 0$. This construction allows one to take the initial condition to be $c(x, t=0) = 0$, which greatly simplifies all calculations.

Effectively, this flux initial condition corresponds to starting the system with the particle at $x = 0$.

As in Sec. 2, we first solve the free theory, where the delta-function term in (14a) is absent, and then use renewal equations to solve the full problem. In the free case, Eq. (14a) becomes, in the Laplace domain:

$$s\tilde{c}_0 + v\partial_x\tilde{c}_0 = D\partial_{xx}\tilde{c}_0, \quad (14b)$$

and is subject to the boundary conditions

$$\begin{cases} (D\partial_x\tilde{c}_0 - v\tilde{c}_0)|_{x=0} = 1 \\ \tilde{c}_0(L, s) = 0, \end{cases}$$

where the subscript 0 denotes the concentration without flux re-injection. The solution to (14b) is standard and the result is (see Appendix B for details):

$$\tilde{c}_0(x, s) = \frac{2e^P \sinh[w(L-x)]}{\mathcal{W}}, \quad (15a)$$

where $P \equiv vx/2D$, $w = \sqrt{v^2 + 4Ds}/2D$ and $\mathcal{W} = 2Dw \cosh(Lw) + v \sinh(Lw)$. In terms of \tilde{c}_0 , the Laplace transform of the first-passage probability to $x = L$ is

$$\tilde{F}_1(L, s) = (-D\partial_x\tilde{c}_0 + v\tilde{c}_0)|_{x=L} = \frac{2Dw e^{Pe}}{\mathcal{W}}, \quad (15b)$$

where again $Pe = vL/2D$ is the Péclet number. With re-injection of the outgoing flux, the concentration obeys the renewal equations. In the Laplace domain and using \tilde{c}_0 above from the free theory, we obtain

$$\tilde{c}(x, s) = \frac{\tilde{c}_0(x, s)}{1 - F_1(L, s)} = \frac{2e^P \sinh[w(L-x)]}{\mathcal{W} - 2Dw e^{Pe}}, \quad (16)$$

where we substitute in the results from Eqs. (15) to obtain the final result.

Contrary to the semi-infinite case, a stationary distribution is attained on the finite interval. To determine this steady state, we use the duality between the limits $s \rightarrow 0$ in the Laplace domain and $t \rightarrow \infty$ in the time domain. With this approach, the coefficient of the term proportional to $1/s$ in $\tilde{c}(x, s)$ gives the steady-state concentration, c_{ss} , in the time domain:

$$c_{ss}(x) \simeq \frac{1}{L} \times \frac{1 - e^{-2(Pe-P)}}{1 - Pe^{-1} e^{-Pe} \sinh(Pe)}, \quad (17)$$

from which the normalized first moment in the steady state is

$$\frac{\langle x \rangle}{L} = \frac{1}{L} \int_0^L x c(x) dx = \frac{(2Pe^2 - 2Pe + 1) e^{2Pe} - 1}{2Pe [(2Pe - 1) e^{2Pe} + 1]}. \quad (18)$$

Representative plots of the stationary-state concentration for different Péclet numbers are given in Fig. 4. As one might anticipate, the density profile is concentrated near

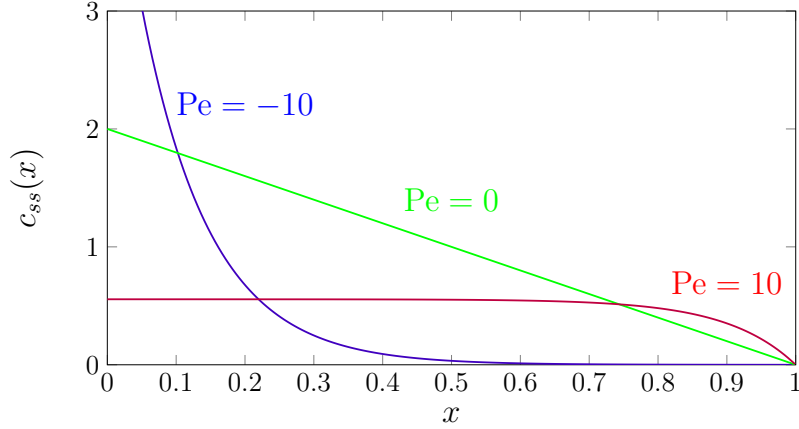


Figure 4. The stationary distribution for the first-passage resetting process on the interval $[0, 1]$ for different Péclet numbers.

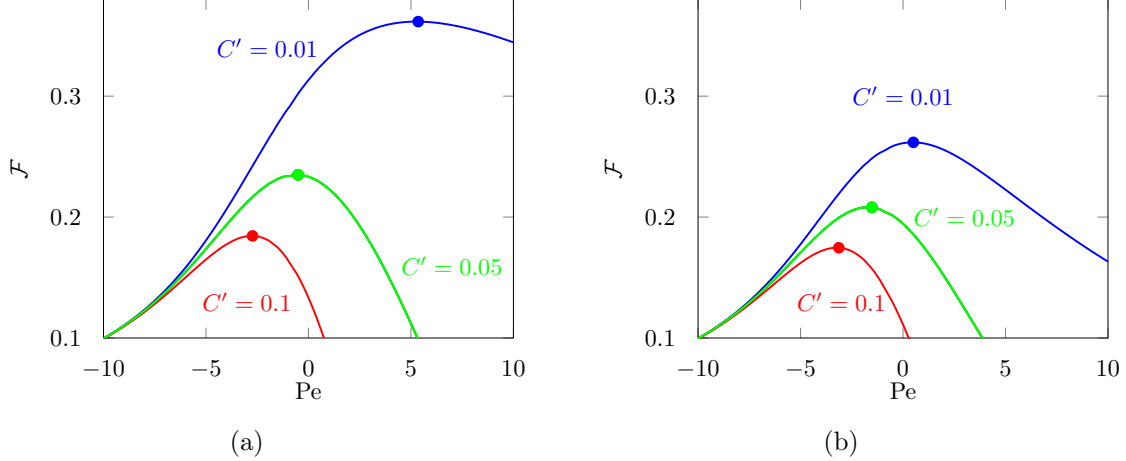


Figure 5. The objective function versus Péclet number Pe for different normalized cost values $C' \equiv C/(L^2/D)$ for: (a) no delay upon resetting, and (b) a dimensionless delay time of $\bar{\tau} = 0.1$ at each resetting. Indicated on each curve is the optimal operating point.

$x = 0$ for negative drift velocity, while for positive drift there is a constant cycling of outgoing flux that is reinjected at $x = 0$, which leads to a nearly constant density profile.

The average number of reset events \mathcal{N} satisfies the renewal equation (A.7a), and substituting in \tilde{F}_1 from (15b), we obtain

$$\tilde{\mathcal{N}}(s) = \frac{2Dw e^{\text{Pe}}}{s [\mathcal{W} - 2Dw e^{\text{Pe}}]}. \quad (19a)$$

We now extract the long-time behavior for the average number of times that $x = L$ is reached by taking the limit $s \rightarrow 0$ of $\tilde{\mathcal{N}}(s)$ to give

$$\mathcal{N}(T) \simeq \frac{4\text{Pe}^2}{2\text{Pe} - 1 + e^{-2\text{Pe}}} \frac{T}{L^2/D}. \quad (19b)$$

Substituting these expressions for $\langle x \rangle/L$ and \mathcal{N} into (13) immediately gives the objective function, and representative plots are shown in Fig. 5(a). For a given cost of a breakdown, there is an optimal drift velocity or optimal Péclet number. The higher this cost, the smaller the optimal bias and the value of \mathcal{F} . Moreover, the optimal bias is not necessarily negative. Indeed, if the cost of a breakdown is relatively small, then it is advantageous to operate the system close to its limit L and absorb the (small) cost of many breakdowns. On the contrary, if the cost of a breakdown is high, it is better to run the system at low level and with a negative bias to avoid breakdowns.

3.2. Time delay for repair

When a mechanical system breaks down, there is usually some downtime during which repairs are made before the system can be restarted. Such a downtime can naturally be incorporated into our model by including a random delay time after each resetting event. Thus when the particle reaches $x = L$ and is returned to $x = 0$, we posit that the particle waits at the origin for a random time τ that is drawn from the exponential distribution $\sigma^{-1}e^{-\tau/\sigma}$ before the particle starts moving again. We now determine the role of this delay on the optimal operation of the system.

The governing renewal equations can be readily extended to incorporate this delay. This delay mechanism can also be viewed as the so-called “sticky” Brownian motion [40–42] that is then combined with first-passage resetting. When we include this delay, the renewal equation for the probability distribution becomes:

$$P(x, t) = G(x, L, t) + \int_0^t dt' F_1(t') \left[\delta_0(x) e^{-(t-t')/\sigma} + \int_0^{t-t'} \frac{d\tau}{\sigma} e^{-\tau/\sigma} P(x, t-t'-\tau) \right]. \quad (20a)$$

This equation encapsulates the two possibilities for the subsequent behavior of the particle when it first reaches $x = L$ at time t' . Either the particle remains at $x = 0$ for the remaining time $t - t'$ or the particle waits for a time $\tau < t - t'$ and then the process starts anew from $(x, t) = (0, t' + \tau)$ for the remaining time $t - t' - \tau$.

In a similar fashion, the renewal equation for the average number of resetting events is

$$\mathcal{N}(t) = \int_0^t dt' F_1(t') \left\{ e^{-(t-t')/\sigma} + \int_0^{t-t'} \frac{d\tau}{\sigma} e^{-\tau/\sigma} [1 + \mathcal{N}(t-t'-\tau)] \right\}. \quad (20b)$$

Equation (20b) accounts for the particle first hitting L at time t' and either waiting at the origin for the entire remaining time $t - t'$ or waiting there for a time $\tau < t - t'$ and then renewing the process for the remaining time. For this latter possibility, there will be, on average, $1 + \mathcal{N}(t - t' - \tau)$ resetting events.

Solving Eqs. (20) in the Laplace domain yields:

$$\begin{aligned} \tilde{P}(x, s) &= \frac{\delta(x) \sigma \tilde{F}_1(s) + \tilde{G}(x, s)(1 + \sigma s)}{1 - F_1(s) + \sigma s}, \\ \tilde{\mathcal{N}}(s) &= \frac{\tilde{F}_1(s)(\sigma + 1/s)}{1 + \sigma s - \tilde{F}_1(s)}. \end{aligned} \quad (21a)$$

We now use the results from Sec. 3.1 for the optimization problem on the interval with no delay. Namely, we substitute in Eqs. (21a) the first-passage probability $\tilde{F}_1(s)$ from Eq. (15b) and the probability distribution in Eq. (15a) for $\tilde{G}(x, s)$ to obtain

$$\begin{aligned}\tilde{P}(x, s) &= \frac{\delta(x) \sigma 2Dw + 2 \sinh(w(L-x))(1 + \sigma s)}{\mathcal{W}e^{-\text{Pe}}(1 + \sigma s) - 2Dw}, \\ \tilde{\mathcal{N}}(s) &= \frac{2Dw(\sigma + 1/s)}{\mathcal{W}e^{-\text{Pe}}(1 + \sigma s) - 2Dw}.\end{aligned}\tag{21b}$$

From the Laplace transform of the spatial probability density, we compute its stationary distribution by taking the $s \rightarrow 0$ limit and obtain

$$P(x) \simeq \frac{e^{\text{Pe}} \text{Pe} (2\bar{\tau} \text{Pe} L \delta_0(x) + 1) - \text{Pe} e^{\text{P}}}{e^{\text{Pe}} (\bar{\tau} \text{Pe}^2 + \text{Pe} - 1) + 1} \frac{1}{L},\tag{22a}$$

where $\bar{\tau} = D\sigma/L^2$ is the dimensionless delay time. From this distribution, the average position of the particle is

$$\frac{\langle x \rangle}{L} = \frac{[(\text{Pe} - 2)\text{Pe} + 2] e^{\text{Pe}} - 2}{2 [\text{Pe}(\bar{\tau} \text{Pe}^2 + \text{Pe} - 1)e^{\text{Pe}} + \text{Pe}]}. \tag{22b}$$

Similarly, the average number of resetting events, or equivalently, the average number of breakdowns in the long-time limit is

$$\mathcal{N} = \frac{\text{Pe}^2}{\text{Pe} - 1 + \bar{\tau} \text{Pe}^2 + e^{-\text{Pe}}} \frac{T}{L^2/D}.\tag{23}$$

These two results, when substituted into Eq. (13), give an objective function \mathcal{F} whose qualitative features are similar to the case of no delay (Fig. 5(b)). This behavior is what might anticipate, since delay may be viewed as an additional form of cost.

The primary difference with the no-delay case is that the optimal Péclet number and the corresponding optimal objective function \mathcal{F} both decrease as the delay time is increased (Fig. 5). Indeed, delay reduces the number of resetting events/breakdowns, but also induces the coordinate to remain closer to the origin. In the limit where the delay is extremely long, the optimal Péclet number will be small. Moreover this optimal value will be nearly independent of the cost per breakdown, as the particle will almost never hit the resetting boundary.

3.3. Two dimensions

It is natural to extend the optimization problem on the interval to higher-dimensional domains. Here, we treat the case where the domain is an annulus of outer radius L , inner radius $a < L$, and the diffusing particle is reset to $r = a$ whenever the outer domain boundary is reached. In analogy with the one-dimensional problem, the particle also experiences drift velocity $v(r) = v_0/r$. As we shall see, the choice of a potential flow field is convenient because the velocity can be combined with the centrifugal term

in the Laplacian, which simplifies the form of the solution. The finite inner radius is needed to eliminate the infinite-velocity singularity that would occur if the inner radius was zero.

In close analogy with the finite-interval system, Eq. (14a), the equation of motion for the particle is

$$\partial_t c + \frac{v}{r} \partial_r c = D \left(\partial_{rr} c + \frac{1}{r} \partial_r c \right) + \delta_a(r) [2\pi r (-D \partial_r c + v c)] \Big|_{r=L}. \quad (24)$$

Here, the flux term has a factor $2\pi r$ due to an integration over all angles. In this geometry, the probability density of finding a particle at a radius r is $2\pi r c(r, t)$. We now introduce the dimensionless variables $x = r/L$, $x_0 = a/L$, the Fourier number $\text{Fo} = Dt/L^2$, and $\text{Pe} = v_0/D\ddagger$ to transform Eq. (24) into

$$\partial_{\text{Fo}} c(x, \text{Fo}) = \partial_{xx} c(x, \text{Fo}) + \frac{1 - \text{Pe}}{x} \partial_x c(x, \text{Fo}) + \delta_{x_0}(x) [2\pi x (-\partial_x c + \text{Pe} c)] \Big|_{x=1}, \quad (25)$$

and the appropriate boundary conditions for this equation are

$$\begin{cases} [\text{Pe} c(x, \text{Fo}) - x \partial_x c(x, \text{Fo})] \Big|_{x=x_0} = \delta(\text{Fo})/(2\pi) \\ c(1, \text{Fo}) = 0 \\ c(x, 0) = 0. \end{cases}$$

By performing similar calculations as in the one-dimensional case we find the following expression for the steady-state probability density in the time domain (see Appendix C for the details):

$$2\pi x c(x) \simeq \frac{2(\text{Pe} + 2)x (x^{\text{Pe}} - 1)}{\text{Pe} (x_0^2 - 1) - 2x_0^2 (x_0^{\text{Pe}} - 1)}. \quad (26)$$

From this expression, the average radial displacement is

$$\langle x \rangle = \int_{x_0}^1 x 2\pi x c(x) dx = \frac{2(\text{Pe} + 2) [\text{Pe} (x_0^3 - 1) - 3x_0^3 (x_0^{\text{Pe}} - 1)]}{3(\text{Pe} + 3) [\text{Pe} (x_0^2 - 1) - 2x_0^2 (x_0^{\text{Pe}} - 1)]}. \quad (27)$$

The average number of reset events \mathcal{N} satisfies a renewal equation and using \tilde{F}_1 from Eq. (C.5) we find

$$\tilde{\mathcal{N}}(s) = \frac{1}{s} \frac{1}{\mathcal{W} - 1}, \quad (28a)$$

where

$$\mathcal{W} = x_0^{1+\text{Pe}/2} \sqrt{s} [K_{\text{Pe}/2}(\sqrt{s}) I_{1+\text{Pe}/2}(\sqrt{s}x_0) + I_{\text{Pe}/2}(\sqrt{s}) K_{1+\text{Pe}/2}(\sqrt{s}x_0)],$$

\ddagger Note that v_0 has units of velocity times length, so this definition of the Péclet number is dimensionally correct.

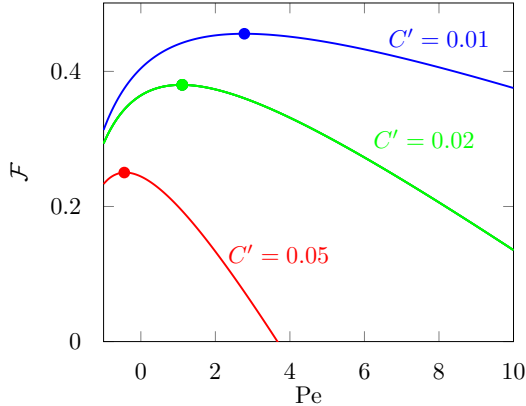


Figure 6. The objective function versus Péclet number Pe for different normalized cost values $C' \equiv C/(L^2/D)$ in two dimensions.

and $I_\nu(x)$ and $K_\nu(x)$ are the modified Bessel functions of the first and second kind, respectively. We now extract the long-time behavior for the average number of times that $x = L$ is reached by taking the limit $s \rightarrow 0$ of $\tilde{\mathcal{N}}(s)$. We find

$$\mathcal{N}(t) \simeq \frac{2Pe(Pe + 2)}{Pe + 2x_0^2(x_0^{Pe} - 1) - Pe x_0^2} Fo. \quad (28b)$$

From Eqs. (27) and (28b), we immediately obtain the objective function and representative results are given in Fig. 6. Overall, the two-dimensional system has the same qualitative behavior as in one dimension. In the limit $x_0 \rightarrow 0$ the average particle position $\langle x \rangle$ and the average number of resetting events \mathcal{N} take an even simpler form than in one dimension:

$$\langle x \rangle \simeq \frac{2(Pe + 2)}{3(Pe + 3)} \Theta(Pe + 2), \quad (29)$$

$$\mathcal{N}(T) \simeq 2(2 + Pe) \Theta(Pe + 2) Fo, \quad (30)$$

where $\Theta(x)$ is the Heaviside step function. The step function arises because of the curious feature that when $Pe < -2$, the flow field Pe/r at the origin is so strong that the particle remains trapped there forever.

4. Domain Growth by First-Passage Resetting

We now turn to a different aspect of first-passage resetting—the growth of a domain as a result of a diffusing particle that reaches the resetting boundary and causes this boundary to recede by a specified amount at each resetting event. Moving boundaries typically arise at the interface between two thermodynamic phases that undergo a first-order phase transition [43, 44]. In this case, the interface moves continuously as the stable phase grows into the unstable phase. A simple example is water freezing at the interface between water and air, when the air temperature is held below 0°C . A layer of ice grows on top of the water as heat is transported away from the ice-water interface.

In these types of systems, the temperature field evolves by diffusion and the movement of the interface is determined by the heat flow at the interface.

In contrast, for a growth process that is induced by first-passage resetting, a single diffusing particle is discontinuously reset to a distant location when the boundary is reached. Concomitantly, the motion of the interface is intermittent and discontinuous when the interface recedes by a finite distance upon hitting. A related behavior also occurs in the absence of resetting: returning to the situation depicted in Fig. 2 (a), a boundary that is initially at L moves to $2L$ when it is hit, and then to $3L$, etc. This interface position clearly moves discontinuously and its position moves as $\sqrt{4Dt/\pi}$.

In the next paragraphs, we study the interface motion and related properties in the presence of first-passage resetting, when the domain of interest is either the semi-infinite line or the finite interval. We find a variety of growth laws that depend on how far the boundary recedes at each resetting event.

4.1. Expanding Semi-Infinite Geometry

Suppose that the diffusing particle starts at the origin and diffuses in the range $[-\infty, L_n]$, with $L_n > 0$. Each time the particle reaches L_n , the particle is reset to the origin and the interface moves forward by a specified amount δL_n so that $L_{n+1} = L_n + \delta L_n$. Since the resetting events occur at separated discrete times, it is convenient to index the position of the interface by n , the number of resetting events. We consider two natural cases: additive and multiplicative interface growth.

4.1.1. Additive growth: $L_n = L_{n-1} + L$. In this case, the right boundary starts at L and then moves to $2L$ at the first reset event, then to $3L$, etc. We make use of the simple relation between diffusion with resetting and free diffusion as shown in Fig. 2. By this equivalence, the probability for n reset events to occur in the time range $[0, t]$ equals the probability that free diffusion travels further than $L_n = n(n+1)L/2$ but no further than $L_{n+1} = (n+1)(n+2)L/2$ in $[0, t]$; that is, the maximum of the freely diffusing particle is located in the range $[L_n, L_{n+1}]$. So, writing again $\mathcal{M}(t)$ for the average of the maximum $M(t)$, one has

$$\sum_{n \geq 0} L_n P(N(t) = n) \leq \sum_{n \geq 0} \int_{L_n}^{L_{n+1}} dm m P(M(t) = m) \leq \sum_{n \geq 0} L_{n+1} P(N(t) = n) ,$$

that is

$$\sum_{n \geq 0} L_n P(N(t) = n) \leq \mathcal{M}(t) \leq \sum_{n \geq 0} L_{n+1} P(N(t) = n) . \quad (31)$$

This leads to

$$\frac{L}{2} [\langle N^2 \rangle + \langle N \rangle] \leq \mathcal{M}(t) \leq \frac{L}{2} [\langle N^2 \rangle + 3 \langle N \rangle + 2] , \quad (32)$$

where we write N for $N(t)$ to simplify the notation, from which it follows that

$$\langle N^2 \rangle \simeq 4\sqrt{\frac{Dt}{\pi L^2}} \quad \text{or} \quad \sqrt{\langle N^2 \rangle} \simeq 2 \left[\frac{Dt}{\pi L^2} \right]^{\frac{1}{4}} \quad (33)$$

Note that we do not obtain directly the average number of reset events $\mathcal{N}(t) \equiv \langle N \rangle$ from (33), but only that it scales as $t^{1/4}$. However, we can derive $\mathcal{N}(t)$ by exploiting the renewal structure of the problem in the Laplace domain (see Appendix D) and find

$$\mathcal{N}(t) \simeq \sqrt{\frac{\pi}{2}} \frac{1}{\Gamma(5/4)} \times \left(\frac{t}{\tau} \right)^{1/4}, \quad (34)$$

where $\tau = L^2/D$ is the diffusion time.

The $t^{1/4}$ scaling is to be compared with the $t^{1/2}$ scaling when the boundary is moving through first-passage dynamics but without resetting. When resetting occurs, the number of encounters with the boundary is reduced because after each reset, the boundary is further away. As one might expect, this boundary recession leads to an anomalously slow interface growth.

4.1.2. Multiplicative growth: $L_n = \alpha L_{n-1}$, $\alpha > 1$. The approach given above can be applied to multiplicative interface recession. That is, upon the first resetting, the initial boundary at $x = L$ moves to $x = \alpha L$. In the next resetting, the boundary moves from $x = \alpha L$ to $x = \alpha^2 L$, etc. For this recession rule, Eq. (31) remains valid, with $L_n = \alpha^n L$. Thus, we have

$$\sum_{n \geq 0} \alpha^n L P(N(t) = n) \leq \mathcal{M}(t) \leq \sum_{n \geq 0} \alpha^{n+1} L P(N(t) = n), \quad (35)$$

from which

$$\langle \alpha^N \rangle L \leq \mathcal{M}(t) \leq \langle \alpha^{N+1} \rangle L. \quad (36)$$

These inequalities suggest that $\mathcal{N}(t)$ scales as $\ln(t/\tau) / 2 \ln \alpha$. From the exact Laplace transform approach (see Appendix D), we also find the same prefactor in the scaling of $\mathcal{N}(t)$ with t . Thus we conclude that

$$\mathcal{N}(t) \simeq \ln(t/\tau) / 2 \ln \alpha. \quad (37)$$

After n resets, the boundary is located at $\alpha^n L$. We also checked numerically that the distribution of $N(t)$ is concentrated sufficiently tightly around its average value $\mathcal{N}(t)$ so that $\langle \alpha^N \rangle \sim \alpha^{\langle N \rangle} = \alpha^{\mathcal{N}(t)}$. As a result, the average position of the boundary at time t scales as

$$\alpha^{\mathcal{N}(t)} L \simeq \sqrt{t/\tau} L. \quad (38)$$

Thus the boundary moves as $t^{1/2}$, which is faster than in the additive case, where the boundary moves as $t^{1/4}$. Despite a smaller number of reset events, each of these moves the boundary far enough for the overall motion to be almost as fast as in the case of first-passage growth without resetting, with the difference being only a factor of 2.

4.2. Expanding Interval

We now study the case where a diffusing particle is confined to a finite and growing interval $[0, L_n]$, with a reflecting boundary condition at $x = 0$. Each time the particle reaches the right boundary at $x = L_n$, the particle is instantaneously reset to $x = 0$, while the position of the boundary recedes by a specified amount. We want to understand how the interval grows with time and related statistical properties of this process. We first give the formal result for an arbitrary dependence of L_n on n and then specialize to the additive case where $L_n = nL$.

We again start with the analog of Eq. (D.1b) for the finite domain, namely, the Laplace transform of the probability to reset for the n^{th} time at t :

$$\tilde{R}_n(s) = \tilde{R}_{n-1}(s) \operatorname{sech}(\sqrt{s/D} L_n) = \prod_{m=1}^n \operatorname{sech}(\sqrt{s/D} L_m). \quad (39)$$

Here $\operatorname{sech}(\sqrt{s/D} L_n)$ is the Laplace transform of the first-passage probability to the right boundary of the finite interval $[0, L_n]$ [25]. Similarly, the average number of resetting events obeys the renewal equation

$$\mathcal{N}(t) = 0 \times Q(L, t) + \sum_{n=1}^{\infty} n \int_0^t dt' Q(L_{n+1}, t - t') R_n(t'), \quad (40a)$$

where $Q(L, t)$ is now the survival probability of a diffusing particle in the finite interval $[0, L_n]$, with reflection at $x = 0$ and absorption at $x = L_n$. In the Laplace domain Eq. (40a) becomes

$$\tilde{\mathcal{N}}(s) = \sum_{n=0}^{\infty} n \tilde{Q}(L_{n+1}, s) \tilde{R}_n(s). \quad (40b)$$

Substituting in $\tilde{Q}(L_n, s) = [1 - \tilde{F}(L_n, s)]/s$ and Eq. (D.1b) into the above equation gives

$$\begin{aligned} \tilde{\mathcal{N}}(s) &= \sum_{n=0}^{\infty} \frac{n}{s} \left[1 - \operatorname{sech}(\sqrt{s/D} L_{n+1}) \right] \prod_{m=1}^n \operatorname{sech}(\sqrt{s/D} L_m) \\ &= \sum_{n=0}^{\infty} \frac{n}{s} \left[\tilde{R}_n(s) - \tilde{R}_{n+1}(s) \right] = \frac{1}{s} \sum_{n=1}^{\infty} \tilde{R}_n(s) \\ &= \frac{1}{s} \sum_{n=1}^{\infty} \prod_{m=1}^n \operatorname{sech}(\sqrt{s/D} L_m) \end{aligned} \quad (41)$$

To extract the asymptotic behavior of $\mathcal{N}(t)$, we now focus on the additive case where $L_n = nL$; that is, the boundary recedes by a fixed distance L after each resetting

event. Using the dimensionless coordinate $\ell = \sqrt{sL^2/D}$, Eq. (41) now gives

$$\begin{aligned}
\tilde{\mathcal{N}}(s) &= \frac{1}{s} \sum_{n=1}^{\infty} \prod_{m=1}^n \operatorname{sech}(\sqrt{s/D} mL) = \frac{1}{s} \sum_{n=1}^{\infty} \prod_{m=1}^n \operatorname{sech}(m\ell) \\
&\approx \frac{1}{s} \sum_{n=1}^{\infty} \exp \left\{ \int_0^n dm \ln [\operatorname{sech}(m\ell)] \right\} \\
&\approx \frac{1}{s} \sum_{n=1}^{\infty} \exp \left\{ -\frac{1}{\ell} \left[-\frac{1}{2} \ell^2 n^2 - \frac{1}{2} \operatorname{Li}_2(-e^{2\ell n}) - \ell n \ln 2 - \frac{\pi^2}{24} \right] \right\} \\
&\approx \frac{1}{s\ell} \int_0^{\infty} du \exp \left\{ -\frac{1}{\ell} \left[-\frac{1}{2} u^2 - \frac{1}{2} \operatorname{Li}_2(-e^{2u}) - u \ln 2 - \frac{\pi^2}{24} \right] \right\}.
\end{aligned}$$

where $\operatorname{Li}_2(x)$ is the polylogarithm function of order 2. This integral can now be computed in the small s limit using the saddle-point approximation (see Appendix E) and the final result is:

$$\begin{aligned}
\tilde{\mathcal{N}}(s) &\approx \frac{1}{s\ell} \int_0^{\infty} du \exp \left(-\frac{u^3}{6} \right) \\
&\approx \Gamma \left(\frac{4}{3} \right) \frac{1}{s} \left(\frac{6}{\ell^2} \right)^{1/3} + o \left(\frac{1}{s^{4/3}} \right).
\end{aligned} \tag{42}$$

The Laplace inversion of the above expression gives the average number of resetting events up to time t in the $t \rightarrow \infty$ limit:

$$\mathcal{N}(t) \simeq \left(\frac{6t}{\tau} \right)^{1/3} + o(t^{1/3}). \tag{43}$$

This result implies that the length of the interval also grows as $t^{1/3}$. For determining the standard deviation (see below), we also need the next correction to the asymptotic behavior. Numerically, we find that $\mathcal{N} \simeq (6t/\tau)^{1/3} + C_1$ where $C_1 = -0.8$.

The $t^{1/3}$ dependence of $\mathcal{N}(t)$ can be understood in a simple way. The mean time for a particle, which starts at $x = 0$, to reach the boundary at $x = L_n$ is $L_n^2/2D = (nL)^2/2D \equiv n^2\tau/2$ [25]. If the particle is immediately reset to the origin each time the boundary is reached, then the time required for \mathcal{N} reset events is $\sum^{\mathcal{N}} n^2\tau/2 \simeq \mathcal{N}^3\tau/6$. This gives $\mathcal{N} \simeq (6t/\tau)^{1/3}$.

The second moment of the probability distribution for the number of encounters is:

$$\langle \tilde{\mathcal{N}}^2(s) \rangle = \sum_{n=0}^{\infty} \frac{n^2}{s} \left[\tilde{R}_n(s) - \tilde{R}_{n+1}(s) \right] = \sum_{n=1}^{\infty} \frac{2n-1}{s} \tilde{R}_n(s) \tag{44}$$

By following similar steps as those to compute \mathcal{N} , we obtain the following result for fixed n and small s :

$$\langle \tilde{\mathcal{N}}^2(s) \rangle \approx \frac{1}{s\ell} \int_0^{\infty} du \left(\frac{2u}{\ell} - 1 \right) \exp \left\{ -\frac{1}{\ell} \left[-\frac{1}{2} u^2 - \frac{1}{2} \operatorname{Li}_2(-e^{2u}) - u \ln 2 - \frac{\pi^2}{24} \right] \right\}.$$

This integral can now be computed in the small- s limit using the saddle-point approximation:

$$\begin{aligned} \langle \tilde{N}^2(s) \rangle &\approx \frac{1}{s\ell} \int_0^\infty du \left(\frac{2u}{\ell} - 1 \right) \exp\left(-\frac{\ell u^3}{6}\right) \\ &\approx \Gamma\left(\frac{5}{3}\right) \frac{1}{s} \left(\frac{6}{\ell^2}\right)^{2/3} + o\left(\frac{1}{s^{5/3}}\right). \end{aligned} \quad (45)$$

Performing a Laplace inversion of the above expression gives:

$$\langle \mathcal{N}^2(t) \rangle \simeq \left(\frac{6t}{\tau}\right)^{2/3} + o(t^{2/3}). \quad (46)$$

Numerically, we find that the next correction is $C_2 (6t/\tau)^{1/3}$ with $C_2 \approx -1.47$. Hence, the standard deviation grows as $\sqrt{\langle \mathcal{N}^2(t) \rangle - \langle \mathcal{N}(t) \rangle^2} \approx \sqrt{C_2 - 2C_1} (6t/\tau)^{1/6}$.

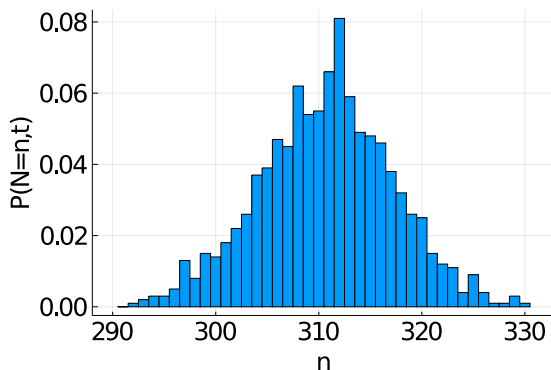


Figure 7. Numerical simulation results for $P(N = n, t)$ for the expanding interval. The initial interval length $L = 1$ and the length grows by 1 after each resetting event. The distribution is shown at $t = 10^9$ for 1000 walkers. The diffusion constant was set to $\Delta x^2/(2\Delta t) = 5 \times 10^{-3}$.

Numerical simulations of this growth process (Fig. 7) show that the distribution of $\mathcal{N}(t)$ is highly localized around its average value and decreases rapidly as one moves away from the maximum. While we do not know how to compute the full distribution analytically, we can determine the tails of the distribution by a simple extremal argument [45, 46]. For notational simplicity we take $L = 1$ and $D = 1$. From the time dependence of the average value of $\mathcal{N}(t)$ (Eq. (43)), we posit that the natural scaling variable is $z \equiv n/\mathcal{N}(t) \simeq n/t^{1/3}$. We further assume that the distribution can be expressed in the scaling form $P(N = n, t) \propto f(z)$ that decays as a stretched exponential for both $z \rightarrow \infty$ and $z \rightarrow 0$. That is, $f(z) = \exp(-z^a)$, where $a > 0$, for $z \rightarrow \infty$ and $f(z) = \exp(-z^b)$, where $b < 0$, for $z \rightarrow 0$.

Consider now the extreme event in which the particle always moves towards the resetting boundary up to time t . This event occurs with probability $2^{-t} \sim e^{-t}$. For this directed motion, the particle requires 1 time step to first reach the boundary, 2 time steps to reach it for a second time, 3 time steps for a third time, etc. This leads to

the total number n of encounters with the boundary that is determined by $\sum_{k=1}^n k = t$. Hence, $n \simeq \sqrt{2t}$. In terms of our scaling function, the probability to reach the boundary $\sqrt{2t}$ times occurs with probability $e^{-t^{a/6}}$. Equating this with e^{-t} gives $a = 6$.

For the small- z tail, we focus on the situation where the boundary is encountered as little as possible. This extremal event is achieved by a random walk that alternately and deterministically moves one step left, then one step right, etc. In the case the boundary is encountered once and only once. This event again occurs with probability $2^{-t} \simeq e^{-t}$. On the other hand, this event of a single boundary encounter corresponds to the scaling variable $z = 1/t^{1/3} \rightarrow 0$, and thus occurs with probability $e^{-t^{-b/3}}$. Equating these two asymptotic forms of the distribution gives $b = -3$. In summary, we find the following asymptotics:

$$P(N = n, t) \simeq \begin{cases} e^{-(n/\mathcal{N}(t))^6} & n \rightarrow \infty, \\ e^{-(n/\mathcal{N}(t))^{-3}} & n \rightarrow 0. \end{cases} \quad (47)$$

Because the exponent values in the scaling forms are fairly large, it does not seem possible to verify these asymptotic behaviors numerically.

5. Summary and Discussion

We presented the concept of first-passage resetting, in which a random walk is reset to its starting point whenever it reaches a specified location. This situation contrasts with constant-rate resetting in which a random walk is reset to its starting point at a fixed rate. In the simple case of a semi-infinite line, $[-\infty, L]$ with $L > 0$, the particle diffuses freely and is reset to the origin whenever it reaches L . The resulting probability distribution has dramatically different behavior depending on whether $0 < x < L$ or $x < 0$. In the former case, the distribution has a simple linear profile that arises from the balance between flux leaving at the reset point and the flux being reinjected at $x = 0$. In the latter case, the probability distribution reduces to free diffusion in the presence of a reflecting boundary. We derived this result analytically and also via a path decomposition that is reminiscent of the image method.

In the finite interval geometry, we defined an optimization problem that describes, in a schematic way, aspects of the repeated breakdown of a driven mechanical system. The operation domain of the system is a finite interval; this interval could be interpreted as the RPM range of an engine. The resetting boundary corresponds the system reaching its operating limit or maximum RPMs, after which a breakdown occurs and the system has to be restarted from scratch. The control parameter is the bias velocity (not to be confused with the RPM of the engine), which may either drive the system towards breakdown or towards minimal-level operation. We showed that there exists an optimal bias velocity that optimizes the performance of the system. This optimum balances the gain by operating close to $x = L$ while minimizing the number of breakdowns. A similar physical picture arises if breakdown is accompanied by a random delay before restarting the system or by extending to a two-dimensional geometry.

We also studied a variety domain growth phenomena that are driven by first-passage dynamics with resetting. When each resetting event moves the boundary by a fixed amount, the boundary recedes as $t^{1/4}$ and as $t^{1/3}$ for the semi-infinite geometry and the finite interval, respectively. In the semi infinite geometry, if the boundary position grows by a factor $\alpha > 1$ with each resetting event, then the interface moves much more quickly, as $t^{1/2}$. The case where the boundary moves by a fixed amount at each resetting is actually a version of the internal diffusion-limited aggregation problem for which there is extensive literature that has focused on the geometrical properties of the growing domain (see, e.g., [47–50]). We instead focused on the rich dynamical aspects of the model and we suggest, based on the correspondence with internal diffusion-limited aggregation, that it will be worthwhile to treat our first–passage resetting in a finite two-dimensional domain.

There are a variety of extensions of the optimization problem may be worth exploring. First, the control strategy could be finer than simply a uniform bias velocity [51]. More realistically, one could also associate a cost to a strategy that becomes more expensive as the control mechanism becomes more sophisticated. For instance, it would be natural to turn on a bias velocity *away* from the breakdown point when the system is very close to breakdown. It would also be useful to identify the optimal region over which the particle experiences a bias (both toward and away from the breakdown point). In addition to a more refined control strategy, other simple geometries may be worthwhile to study. One such example is a one-dimensional interval with a first-passage resetting mechanism at each end of the interval and with a different cost in reaching each end. First-passage resetting in a bounded planar geometry with a cost function that depends on the hitting angle of the boundary might be another geometry that will be worthwhile to study.

Given the rich behavior exhibited by first-passage resetting, it should also be worthwhile to investigate both extensions of the basic model and applications. An example of the former is the Fleming-Viot branching process, in which there are $N + 1$ particles and when one of them resets, it resets to one of the positions of the remaining N particles [52–56]. More generally, the first-passage resetting in the presence of multiple diffusing particles could lead to new phenomenology. On another note, applications also exist in cash flow management: cash levels in a large firm are sometimes modeled as a diffusion process in which one wishes to have cash fully invested in profitable ventures, while at the same time keeping enough cash available so as to avoid being indebted [57, 58]. These types of problems seem to be ripe for further exploration.

6. Acknowledgments

BBs research at the Perimeter Institute was supported in part by the Government of Canada through the Department of Innovation, Science and Economic Development Canada and by the Province of Ontario through the Ministry of Colleges and Universities. JRFs research at Columbia University was supported by the Alliance

Program. SR thanks Paul Hines for helpful conversations and financial support from NSF grant DMR-1910736. We thank one of the referees for providing helpful suggestions about possible extensions of the basic optimization problem.

Appendix A. Laplace transform approach in the semi-infinite geometry

Appendix A.1. Spatial probability distributions

The probability distribution $P(x, t)$ of the diffusing particle at time t on the semi-infinite line $x \leq L$, can be obtained in several ways. We presented in the main text a path transformation approach and we detail here the Laplace transform approach (see also [34]). We first partition the trajectory according to the number of reset events up to time t . Between consecutive resets, the particle undergoes free diffusion with an absorbing boundary at $x = L$. This part of the motion is described by the free propagator

$$G(x, L, t) = [e^{-x^2/4Dt} - e^{-(x-2L)^2/4Dt}] / \sqrt{4\pi Dt}, \quad (\text{A.1})$$

which can be computed, for example, by the image method [24, 25]. Summing over all numbers of reset events, the spatial probability is determined by

$$P(x, t) = G(x, L, t) + \sum_{n \geq 1} \int_0^t dt' F_n(L, t') G(x, L, t-t'). \quad (\text{A.2a})$$

Equation (A.2a) states that for the particle to be at x at time t , it either: (i) must never hit L , in which case its probability distribution is just $G(x, L, t)$, or (ii), the particle first hits L for the n^{th} time at $t' < t$, after which the particle restarts at the origin and then propagates to x in the remaining time $t - t'$ without hitting L again. The equivalent way of writing Eq. (A.2a) in a renewal fashion is:

$$P(x, t) = G(x, L, t) + \int_0^t dt' F_1(L, t') P(x, t-t'). \quad (\text{A.2b})$$

The first term accounts for the particle never reaching $x = L$, while the second term accounts for the particle reaching $x = L$ at time t' , after which the process starts anew from $x(t') = 0$ for the remaining time $t - t'$. Note that this is a renewal equation in the sense that the second term contains the full propagator $P(x, t-t')$ and not the free propagator $G(x, t-t')$, thereby accounting for any number of resetting events in the time interval $[t', t]$.

To solve for $P(x, t)$ we again treat the problem in the Laplace domain. While we can find the solution from the Laplace transform of Eq. (A.2a), the solution is simpler and more direct from the Laplace transform of (A.2b):

$$\tilde{P}(y, s) = \tilde{G}(y, \ell, s) + \tilde{F}_1(\ell, s) \tilde{P}(y, s), \quad (\text{A.3a})$$

with

$$\tilde{G}(y, \ell, s) = [e^{-|y|} - e^{-|y-2\ell|}] / \sqrt{4Ds},$$

the Laplace transform of $G(x, L, t)$, where we have introduced the scaled coordinates $y \equiv x\sqrt{s/D}$ and $\ell \equiv L\sqrt{s/D}$. Solving for $\tilde{P}(y, s)$ yields:

$$\tilde{P}(y, s) = \frac{\tilde{G}(y, \ell, s)}{1 - \tilde{F}_1(\ell, s)} = \frac{1}{\sqrt{4Ds}} \frac{[e^{-|y|} - e^{-|y-2\ell|}]}{1 - e^{-\ell}}. \quad (\text{A.3b})$$

To invert this Laplace transform, we separately consider the cases $0 \leq y \leq \ell$ and $y < 0$. In the former, we expand the denominator in a Taylor series to give

$$\begin{aligned} \tilde{P}(y, s) &= \frac{1}{\sqrt{4Ds}} [e^{-y} - e^{-(2\ell-y)}] \sum_{n \geq 0} e^{-n\ell} \\ &= \frac{1}{\sqrt{4Ds}} \sum_{n \geq 0} [e^{-(y+n\ell)} - e^{-[(n+2)\ell-y]}], \quad 0 < y \leq \ell, \end{aligned} \quad (\text{A.4a})$$

from which

$$P(x, t) = \frac{1}{\sqrt{4\pi Dt}} \sum_{n \geq 0} [e^{-(x+nL)^2/4Dt} - e^{-[x-(n+2)L]^2/4Dt}], \quad 0 < x \leq L. \quad (\text{A.4b})$$

In the case of $y < 0$, $\tilde{P}(y, s)$ in Eq. (A.3b) is factorizable:

$$\tilde{P}(y, s) = \frac{1}{\sqrt{4Ds}} \left[\frac{e^y - e^{y-2\ell}}{1 - e^{-\ell}} \right] = \frac{1}{\sqrt{4Ds}} [e^y + e^{(y-\ell)}], \quad (\text{A.5a})$$

and this latter form can be readily inverted to give:

$$P(x, t) = \frac{1}{\sqrt{4\pi Dt}} [e^{-x^2/4Dt} + e^{-(x-L)^2/4Dt}] \quad x < 0. \quad (\text{A.5b})$$

Appendix A.2. Average number of resets

The average number of resets that occur up to time t may also be derived by using the Laplace transform approach. The probability for n resets to occur by time t equals the probability to have at least n resets minus the probability to have at least $n+1$ resets:

$$\begin{aligned} P(N(t)=n) &= P(N(t) \geq n) - P(N(t) \geq n+1), \\ &= \int_0^t dt' F_n(L, t') - \int_0^t dt' F_{n+1}(L, t'). \end{aligned} \quad (\text{A.6a})$$

Using our earlier result that $F_n(L, t) = F_1(nL, t)$, we have

$$P(N(t)=n) = \text{erf}\left(\frac{(n+1)L}{\sqrt{4Dt}}\right) - \text{erf}\left(\frac{nL}{\sqrt{4Dt}}\right), \quad (\text{A.6b})$$

where erf is the Gauss error function.

We can compute the average number of reset events, $\mathcal{N}(t) \equiv \langle N(t) \rangle$, from (7), but it is quicker to use a renewal equation approach. Here we can write

$$\mathcal{N}(t) = \int_0^t dt' F_1(L, t-t') [1 + \mathcal{N}(t')]. \quad (\text{A.7a})$$

Equation (A.7a) states that to have \mathcal{N} reset events up to time t , $\mathcal{N} - 1$ reset events must have occurred at some earlier time $t' < t$ and then one more reset event occurs exactly at time t . Taking the Laplace transform of (A.7a) gives

$$\tilde{\mathcal{N}}(s) = \frac{\tilde{F}_1(L, s)}{s(1 - \tilde{F}_1(L, s))} = \frac{e^{-\ell}}{s(1 - e^{-\ell})}, \quad (\text{A.7b})$$

where again $\ell = L\sqrt{s/D}$. We extract the long-time behavior of the average number of reset events by taking the $s \rightarrow 0$ limit and then Laplace inverting this limiting expression. We thus find

$$\mathcal{N}(t) \simeq \sqrt{4Dt/\pi L^2}. \quad (\text{A.8})$$

Appendix B. Solution to the convection-diffusion equation

The general solution to Eq. (14b) is

$$\tilde{c}_0(x, s) = e^P(Ae^{wx} + Be^{-wx}), \quad (\text{B.1})$$

where $P = vx/2D$, $w = \sqrt{v^2 + 4Ds}/2D$, and A, B are integration constants. To determine A and B , we apply the boundary conditions that accompany Eq. (B.1) to give the linear system

$$\begin{cases} v(A + B) - \frac{1}{2}v(A + B) - ADw + BDw = 1, \\ e^{vL/(2D)}(Ae^{Lw} + Be^{-Lw}) = 0, \end{cases} \quad (\text{B.2})$$

whose solution is

$$\begin{cases} A = -\frac{2}{2Dwe^{2Lw} + 2Dw + ve^{2Lw} - v} = -\frac{e^{-Lw}}{2Dw \cosh(Lw) + v \sinh(Lw)}, \\ B = \frac{2e^{2Lw}}{2Dwe^{2Lw} + 2Dw + ve^{2Lw} - v} = \frac{e^{Lw}}{2Dw \cosh(Lw) + v \sinh(Lw)}. \end{cases} \quad (\text{B.3})$$

We define $\mathcal{W} \equiv 2Dw \cosh(Lw) + v \sinh(Lw)$, from which $A = -e^{-Lw}/\mathcal{W}$ and $B = e^{Lw}/\mathcal{W}$. Substituting these constants back into the general solution Eq. (B.1) leads to Eq. (15a).

Appendix C. First-passage resetting in the annular geometry

For the convection-diffusion equation in two dimensions with a radial drift v/r ; that is, Eq. (25) without the delta-function term, the general solution in the Laplace domain is [59]

$$\tilde{c}_0(x, s) = x^{\text{Pe}/2} [A I_{\text{Pe}/2}(\sqrt{s}x) + B K_{\text{Pe}/2}(\sqrt{s}x)], \quad (\text{C.1})$$

where A , and B are integration constants, and $I_\nu(x)$ and $K_\nu(x)$ are the modified Bessel functions of the first and second kind, respectively. The subscript 0 refers to

the concentration without flux re-injection. Imposing the boundary conditions that accompany Eq. (25) leads to a linear system to solve for A and B :

$$\begin{cases} AI_{\text{Pe}/2}(\sqrt{s}) + BK_{\text{Pe}/2}(\sqrt{s}) & = 0, \\ \sqrt{s}x_0^{1+\text{Pe}/2} (BK_{1+\text{Pe}/2}(\sqrt{s}x_0) - AI_{1+\text{Pe}/2}(\sqrt{s}x)) & = 1/(2\pi). \end{cases} \quad (\text{C.2})$$

whose solution is:

$$\begin{cases} A = -\frac{x_0^{-(1+\text{Pe}/2)} K_{\text{Pe}/2}(\sqrt{s})}{2\pi\sqrt{s} (K_{\text{Pe}/2}(\sqrt{s}) I_{1+\text{Pe}/2}(\sqrt{s}x_0) + I_{\text{Pe}/2}(\sqrt{s}) K_{1+\text{Pe}/2}(\sqrt{s}x_0))}, \\ B = \frac{x_0^{-(1+\text{Pe}/2)} I_{\text{Pe}/2}(\sqrt{s})}{2\pi\sqrt{s} (K_{\text{Pe}/2}(\sqrt{s}) I_{1+\text{Pe}/2}(\sqrt{s}x_0) + I_{\text{Pe}/2}(\sqrt{s}) K_{1+\text{Pe}/2}(\sqrt{s}x_0))}. \end{cases} \quad (\text{C.3})$$

We now define $\mathcal{W} \equiv x_0^{1+\text{Pe}/2} \sqrt{s} [K_{\text{Pe}/2}(\sqrt{s}) I_{1+\text{Pe}/2}(\sqrt{s}x_0) + I_{\text{Pe}/2}(\sqrt{s}) K_{1+\text{Pe}/2}(\sqrt{s}x_0)]$. In terms of this function, we have $A = K_{\text{Pe}/2}(\sqrt{s}) / (2\pi\mathcal{W})$ and $B = I_{\text{Pe}/2}(\sqrt{s}) / (2\pi\mathcal{W})$. Substituting these constants back into Eq. (C.1) yields:

$$\tilde{c}_0(x, s) = \frac{x^{\text{Pe}/2} [I_{\text{Pe}/2}(\sqrt{s}) K_{\text{Pe}/2}(\sqrt{s}x) - K_{\text{Pe}/2}(\sqrt{s}) I_{\text{Pe}/2}(\sqrt{s}x)]}{2\pi\mathcal{W}}, \quad (\text{C.4})$$

The first-passage probability is obtained by computing the outlet flux at $x = 1$ from the concentration in Eq. (C.4):

$$\begin{aligned} \tilde{F}_1(s) &= 2\pi (-x\partial_x \tilde{c}_0(x, s) + \text{Pe} \tilde{c}_0(x, s))|_{x=1} \\ &= 2\pi (-\partial_x \tilde{c}_0(x, s))|_{x=1} \\ &= \frac{\sqrt{s} I_{\text{Pe}/2}(\sqrt{s}) K_{1-\text{Pe}/2}(\sqrt{s}) + \sqrt{s} I_{1-\text{Pe}/2}(\sqrt{s}) K_{\text{Pe}/2}(\sqrt{s})}{\mathcal{W}} = \frac{1}{\mathcal{W}}, \end{aligned} \quad (\text{C.5})$$

where we used the absorbing boundary condition to go to the second line.

On the other hand, the survival probability $Q(t)$ is defined as the integral of $2\pi x \tilde{c}_0(x, t)$ over the interval $[x_0, 1]$. Alternatively, it can be computed as the probability of not having hit the absorbing boundary until time t : $Q(t) = 1 - \int_0^t dt' F_1(t')$, which in the Laplace domain translates to $\tilde{Q}(s) = (1 - \tilde{F}_1(s))/s$. Using Eq. (C.5), we obtain:

$$\tilde{Q}(s) = \frac{1}{s} \left(1 - \frac{1}{\mathcal{W}} \right). \quad (\text{C.6})$$

When there is re-injection of the outgoing flux, the concentration obeys the renewal equation below. In the Laplace domain and using the form for \tilde{c}_0 obtained above, we find:

$$\tilde{c}(x, s) = \frac{\tilde{c}_0(x, s)}{1 - \tilde{F}_1(s)} = \frac{x^{\text{Pe}/2} [I_{\text{Pe}/2}(\sqrt{s}) K_{\text{Pe}/2}(\sqrt{s}x) - K_{\text{Pe}/2}(\sqrt{s}) I_{\text{Pe}/2}(\sqrt{s}x)]}{2\pi(\mathcal{W} - 1)}. \quad (\text{C.7})$$

In the $s \rightarrow 0$ limit, we find that:

$$\begin{aligned} x^{\text{Pe}/2} [I_{\text{Pe}/2}(\sqrt{s}) K_{\text{Pe}/2}(\sqrt{s}x) - K_{\text{Pe}/2}(\sqrt{s}) I_{\text{Pe}/2}(\sqrt{s}x)] &\simeq \frac{1 - x^{\text{Pe}}}{\text{Pe}}, \\ \mathcal{W} - 1 &\simeq \frac{\text{Pe} - \text{Pe} x_0^2 + 2x_0^2 (-1 + x_0^{\text{Pe}})}{2\text{Pe}(2 + \text{Pe})} s. \end{aligned} \quad (\text{C.8})$$

Substituting these asymptotic expressions in Eq. (C.7), the coefficient of the term proportional to $1/s$ in $\tilde{c}(x, s)$ gives the steady-state probability density in the time domain that is quoted in Eq. (26).

Appendix D. Expanding semi-infinite geometry: Laplace transforms

We derive here with Laplace transforms the properties for domain growth in the semi-infinite geometry that was obtained in the main text using a path transformation. Suppose that the diffusing particle starts at the origin and diffuses in the range $[-\infty, L_n]$, with $L_n > 0$. Each time the particle reaches L_n , the particle is reset to the origin and the interface moves forward by a specified amount δL_n so that $L_{n+1} = L_n + \delta L_n$. Since the resetting events occur at separated discrete times, it is convenient to index the position of the interface by n , the number of resetting events. We consider two natural cases: additive and multiplicative interface growth.

Appendix D.1. Additive growth: $L_n = L_{n-1} + L$.

In this case, the right boundary starts at L and then moves to $2L$ at the first reset event, then to $3L$, etc. The probability that the n^{th} reset occurs at time t , $R_n(t)$, is given by the renewal equation

$$R_n(t) = \int_0^t dt' R_{n-1}(t-t') F(L_n = nL, t'), \quad (\text{D.1a})$$

where $F(L_1, t)$ is the standard first-passage probability to reach L_1 when the particle starts from the origin. In the Laplace domain Eq. (D.1a) becomes

$$\tilde{R}_n(s) = \tilde{R}_{n-1}(s) e^{-n\ell} = e^{-n(n+1)\ell/2}, \quad (\text{D.1b})$$

with $\ell \equiv \sqrt{sL^2/D}$.

By similar considerations, the average number of resetting events is

$$\mathcal{N}(t) = 0 \times Q(L, T) + \sum_{n=1}^{\infty} n \int_0^t dt' Q((n+1)L, t-t') R_n(t'), \quad (\text{D.2a})$$

which, in the Laplace domain, becomes

$$\tilde{\mathcal{N}}(s) = \sum_{n=0}^{\infty} n \tilde{Q}((n+1)L, s) \tilde{R}_n(s). \quad (\text{D.2b})$$

Here $Q(L, t) = 1 - \int_0^t dt' F(L, t')$ is the survival probability for a diffusing particle that starts at the origin to not reach an absorbing boundary at L within time T .

In the Laplace domain, this relation becomes $\tilde{Q}(nL, s) = [1 - \tilde{F}(nL, s)]/s$. We now substitute this expression for \tilde{Q} and the above expression for $\tilde{R}_n(s)$ into (D.2b),

and then convert the sum to an integral to give

$$\begin{aligned}
\tilde{\mathcal{N}}(s) &\approx \int_0^\infty dn \frac{n}{s} [1 - e^{-(n+1)\ell}] e^{-n(n+1)\ell/2} \\
&= \frac{e^{-\ell}}{4s\ell} \left\{ \sqrt{2\pi\ell} e^{9\ell/8} [2 + \operatorname{erf}(\sqrt{\ell/8}) - 3 \operatorname{erf}(3\sqrt{\ell/8})] + 4e^\ell - 4 \right\} \\
&\rightarrow \frac{1}{s} \sqrt{\frac{\pi}{2\ell}} \quad s \rightarrow 0.
\end{aligned} \tag{D.3a}$$

Laplace inverting this expression, the average number of reset events asymptotically scales as

$$\mathcal{N}(t) \simeq \sqrt{\frac{\pi}{2}} \frac{1}{\Gamma(5/4)} \times \left(\frac{t}{\tau} \right)^{1/4}, \tag{D.3b}$$

where $\tau = L^2/D$ is the diffusion time.

Appendix D.2. Multiplicative growth: $L_n = \alpha L_{n-1}, \alpha > 1$.

The approach given above can be applied to multiplicative interface recession. That is, upon the first resetting, the initial boundary at $x = L$ moves to $x = \alpha L$. In the next resetting, the boundary moves from $x = \alpha L$ to $x = \alpha^2 L$, etc. For this recession rule, the probability for the n^{th} reset event to occur at time at t , $R_n(t)$, is

$$R_n(t) = \int_0^t dt' R_{n-1}(t-t') F(\alpha^{n-1}L, t'), \tag{D.4a}$$

which, in the Laplace domain, becomes

$$\tilde{R}_n(s) = \tilde{R}_{n-1}(s) e^{-\sqrt{s/D} \alpha^{n-1}L} \equiv \tilde{R}_{n-1}(s) e^{-\ell \alpha^{n-1}} = e^{-\ell(1-\alpha^n)/(1-\alpha)}. \tag{D.4b}$$

The average number of reset events up to time t is

$$\mathcal{N}(t) = 0 \times Q(L, T) + \sum_{n=1}^\infty n \int_0^t dt' Q(\alpha^n L, t-t') R_n(t'), \tag{D.5a}$$

which becomes, in the Laplace domain,

$$\tilde{\mathcal{N}}(s) = \sum_{n=0}^\infty n \tilde{Q}(\alpha^n L, s) \tilde{R}_n(s). \tag{D.5b}$$

Substituting in $\tilde{Q}(\alpha^n L, s) = [1 - \tilde{F}(\alpha^n L, s)]/s$ and (D.4b) into the above equation, we obtain

$$\begin{aligned}
\tilde{\mathcal{N}}(s) &= \sum_{n=0}^\infty \frac{n}{s} (1 - e^{-\ell \alpha^n}) e^{-\ell(1-\alpha^n)/(1-\alpha)} \\
&\approx \int_0^\infty dn \frac{n}{s} (1 - e^{-\ell \alpha^n}) e^{-\ell(1-\alpha^n)/(1-\alpha)} \\
&= \frac{1}{s} e^{-\ell/(1-\alpha)} \int_0^\infty dn n (1 - e^{-\ell \alpha^n}) e^{\ell \alpha^n/(1-\alpha)}.
\end{aligned} \tag{D.6}$$

To evaluate the above integral, we make the variable change $z = \ell \alpha^{n-1}$, from which $n = \ln(z \alpha / \ell) / \ln \alpha$ and $dn = dz / (z \ln \alpha)$. The above integral now becomes:

$$\tilde{\mathcal{N}}(s) = \frac{1}{s} \frac{e^{-\ell/(1-\alpha)}}{(\ln \alpha)^2} \int_{\ell/\alpha}^{\infty} dz \frac{\ln(z \alpha / \ell)}{z} (1 - e^{-\alpha z}) e^{\alpha z / (1-\alpha)},$$

For $s \rightarrow 0$, we compute the above integral by first splitting it into two terms, by using $\ln(z \alpha / \ell) = \ln z + \ln(\alpha / \ell)$. The contribution from the first term is while the second one diverges. Dropping the finite term, we obtain

$$\tilde{\mathcal{N}}(s) \simeq \frac{\ln(\alpha / \ell)}{s} \frac{e^{-\ell/(1-\alpha)}}{(\ln \alpha)^2} \int_{\ell/\alpha}^{\infty} dz \frac{1 - e^{-\alpha z}}{z} e^{\alpha z / (1-\alpha)} \simeq -\frac{\ln(s\tau)}{2 s \ln \alpha}, \quad s \rightarrow 0. \quad (\text{D.7})$$

Note that we introduce the factor τ inside the logarithm, so that this term is manifestly dimensionless. Thus in the long-time limit, the average number of resetting events scales as

$$\mathcal{N}(t) \simeq \frac{\ln(t/\tau)}{2 \ln \alpha}. \quad (\text{D.8})$$

Appendix E. Expanding interval: Saddle point approximation

We want to compute the following integral in the small ℓ limit:

$$I(\ell) = \int_0^{\infty} du \exp\left[-\frac{1}{\ell} f(u)\right], \quad (\text{E.1})$$

where $f(u) = -\frac{1}{2}u^2 - \frac{1}{2}\text{Li}_2(-e^{2u}) - u \log(2) - \frac{\pi^2}{24}$. Because the negative exponential is rapidly decreasing as $\ell \rightarrow 0$, the main contribution will occur when $f(u)$ is minimum. This function has a global minimum located at $u = 0$ and can be locally approximated by $f(u) \simeq u^3/6$. Substituting this into Eq. (E.1), we recover Eq. (42).

References

- [1] Chandrasekhar S 1943 *Rev. Mod. Phys.* **15** 1
- [2] Van Kampen N G 1992 *Stochastic processes in physics and chemistry* vol 1 (Elsevier)
- [3] Chicheportiche R and Bouchaud J P 2014 Some applications of first-passage ideas to finance *First-passage Phenomena And Their Applications* (World Scientific) pp 447–476
- [4] Rogers E M 2010 *Diffusion of innovations* (Simon and Schuster)
- [5] Weiss G H 1994 *Aspects and applications of the random walk* (North Holland)
- [6] Hughes B D *et al.* 1995 *Random walks and random environments: random walks* vol 1 (Oxford University Press)

- [7] Rudnick J and Gaspari G 2004 *Elements of the random walk: an introduction for advanced students and researchers* (Cambridge University Press)
- [8] Klafter J and Sokolov I M 2011 *First steps in random walks: from tools to applications* (Oxford University Press)
- [9] Evans M R and Majumdar S N 2011 *Phys. Rev. Lett.* **106** 160601
- [10] Evans M R and Majumdar S N 2011 *J. Phys. A: Mathematical and Theoretical* **44** 435001
- [11] Evans M R, Majumdar S N and Schehr G 2020 *J. Phys. A: Mathematical and Theoretical* **53** 193001
- [12] Boyer D and Solis-Salas C 2014 *Phys. Rev. Lett.* **112**(24) 240601
- [13] Christou C and Schadschneider A 2015 *J. Phys. A: Mathematical and Theoretical* **48** 285003
- [14] Rotbart T, Reuveni S and Urbakh M 2015 *Phys. Rev. E* **92**(6) 060101
- [15] Majumdar S N, Sabhapandit S and Schehr G 2015 *Phys. Rev. E* **92**(5) 052126
- [16] Reuveni S 2016 *Phys. Rev. Lett.* **116** 170601
- [17] Pal A and Reuveni S 2017 *Phys. Rev. Lett.* **118** 030603
- [18] Belan S 2018 *Phys. Rev. Lett.* **120** 080601
- [19] Bodrova A S, Chechkin A V and Sokolov I M 2019 *Phys. Rev. E* **100** 012119
- [20] Kuśmierz L and Gudowska-Nowak E 2015 *Phys. Rev. E* **92**(5) 052127
- [21] Campos D and Méndez V m c 2015 *Phys. Rev. E* **92**(6) 062115
- [22] Bhat U, De Bacco C and Redner S 2016 *J. Stat. Mech.: Theory and Experiment* **2016** 083401
- [23] Eule S and Metzger J J 2016 *New J. Phys.* **18** 033006
- [24] Feller W 2008 *An introduction to probability theory and its applications* vol 1 (John Wiley & Sons)
- [25] Redner S 2001 *A Guide to First-Passage Processes* (Cambridge University Press)
- [26] Bray A J, Majumdar S N, Schehr G 2015 *Advances in Physics* **62** 225–361
- [27] Feller W 1954 *Trans. Amer. Math. Soc.* **77** 1–31
- [28] Sherman B 1958 *Ann. Math. Stat.* **29** 267–273
- [29] Falcao R and Evans M R 2017 *J. Stat. Mech.: Theory and Experiment* **2017** 023204
- [30] Ross S M 2014 *Introduction to Probability Models* (Academic Press)
- [31] Gnedenko B V, Belyayev Y K and Solovyev A D 2014 *Mathematical methods of reliability theory* (Academic Press)
- [32] Ajjarapu V, Ping Lin Lau and Battula S 1994 *IEEE Transactions on Power Systems* **9** 906–917
- [33] Zhihong Feng, Ajjarapu V and Maratukulam D J 2000 *IEEE Transactions on Power Systems* **15** 791–797

- [34] De Bruyne B, Randon-Furling J and Redner S 2020 *Physical Review Letters* **125** 050602
- [35] Lévy P 1948 *Processus stochastiques et mouvement brownien* (Gauthier-Villars)
- [36] Borodin A N and Salminen P 2012 *Handbook of Brownian motion – Facts and formulae* (Birkhäuser)
- [37] Bachelier L 1900 *Annales scientifiques de l'École normale supérieure* **17** 21–86
- [38] Lévy P 1940 *Compositio mathematica* **7** 283–339
- [39] Krapivsky P and Redner S 2018 *Journal of Statistical Mechanics: Theory and Experiment* **2018** 093208
- [40] Gallavotti G and McKean H 1972 *Nagoya Mathematical Journal* **47** 1–14
- [41] Harrison J M and Lemoine A J 1981 *Journal of Applied Probability* **18** 216–226
- [42] Bou-Rabee N and Holmes-Cerfon M C 2020 *SIAM Review* **62** 164–195
- [43] Crank J 1987 *Free and moving boundary problems* (Oxford University Press)
- [44] Rubinstein L 2000 *The stefan problem* vol 8 (American Mathematical Soc.)
- [45] Fisher M E 1966 *The Journal of Chemical Physics* **44** 616–622
- [46] Krapivsky P L, Redner S and Ben-Naim E 2010 *A kinetic view of statistical physics* (Cambridge University Press)
- [47] Meakin P and Deutch J M 1986 *The Journal of chemical physics* **85** 2320–2325
- [48] Lawler G F, Bramson M and Griffeath D 1992 *The Annals of Probability* 2117–2140
- [49] Moore C and Machta J 2000 *Journal of Statistical Physics* **99** 661–690
- [50] Jerison D, Levine L and Sheffield S 2012 *Journal of the American Mathematical Society* **25** 271–301
- [51] Lunz D 2020 *Journal of Physics A: Mathematical and General* **44** 44LT01
- [52] Fleming W H and Viot M 1979 *Indiana University Mathematics Journal* **28** 817–843
- [53] Burdzy K, Holyst R, Ingerman D and March P 1996 *Journal of Physics A: Mathematical and General* **29** 2633
- [54] Burdzy K, Hołyst R and March P 2000 *Communications in Mathematical Physics* **214** 679–703
- [55] Grigorescu I and Kang M 2004 *Stochastic processes and their applications* **110** 111–143
- [56] Grigorescu I, Kang M *et al.* 2006 *Electronic Journal of Probability* **11** 311–331
- [57] Harrison J M, Sellke T M and Taylor A J 1983 *Mathematics of Operations Research* **8** 454–466
- [58] Buckholtz P G, Campbell L L, Milbourne R D and Wasan M 1983 *Journal of Applied Probability* **20** 61–70
- [59] Abramowitz M, Stegun I A and Romer R H 1988 *Handbook of mathematical functions with formulas, graphs, and mathematical tables*